RECONSTRUCTION OF THE DEFORMATION SURFACE OF CFER PANELS

Forlani G. - Guzzetti F. -Pinto L.
Dip. I.I.A.R. Politecnico di Milano, P.za L. da Vinci n. 32, 20133 Milano Italy
E-Mail gianfra@ipmtf2.topo.polimi.it

Commission 5, Working Group 3

KEY WORDS: Accuracy, Close_Range, Industrial, Matching, Targets, Scanner, Performance

ABSTRACT:

In the framework of a project on modeling by finite elements the mechanical properties of Carbon Fiber Epossy Reinforced panels, a series of tests have been carried out, aiming to determine the deformation surface of the panels under load. The deformations were recovered by a photogrammetric survey, using an analogue camera for image acquisition, then scanning and processing the digital images. This paper reports about the project design and the scanner calibration; the procedure used for semi-automatic target measurement and point transfer is also discussed. The required accuracy for the deformation surface, set around 0.1 mm over the whole panel, has been obtained in all tests.

1. INTRODUCTION

In the aviation industry, research is struggling to reduce the weight of structures and components, while improving or at least preserving their mechanical characteristics. Since still little is known about the behaviour of Carbon Fiber Epossy Reinforced (CFER) elements in post-buckling, they are designed and dimensioned so that the stress never push the element beyond the limit of the elastic state. To overcome this limit and to get a substantial reduction in weight, a deeper understanding of the mechanical behaviour is necessary, which can be achieved by an experimental stage, in static and dynamic mode, performed to tune the parameters of an appropriate finite element model. Once a reliable model is available, detailed analyses may be performed, avoiding the cost of extensive experimentation. A joint operation by the Departments of Aeronautics, Constructions and Surveying of the T.U. of Milan has been carried out, aiming to determine the deformation surface of different panels at various loading stages. Tests have been carried out on CFER and aluminium panels, of about 80x80 cm of size, inserted in a loading machine capable to replicate the same loading and binding conditions experienced in flight (see figure 1). In this initial stage, tests have been performed in static mode only; the effect of dynamic changes, which is the most relevant case, will be addressed later.
Since the number of tests to complete was in the order of tens, attention has been paid to design a procedure which in time will be run by non-photogrammetrists, therefore ensuring a certain level of performance, while at the same time maintaining a simple operational scheme, though there was no commitment to building an integrated fully operational system.
The behaviour of the panel under load is described by the deformations due to bending and by the differences between the initial and the current position at any loading condition.
In order to trace these and other relevant parameters, a number of techniques and sensors may be used. Apart from strain gauges, which are necessary to measure strain and stress in a few critical points, proximity gauges may be put together in arrays or matrices and operated by some precise positioning device.

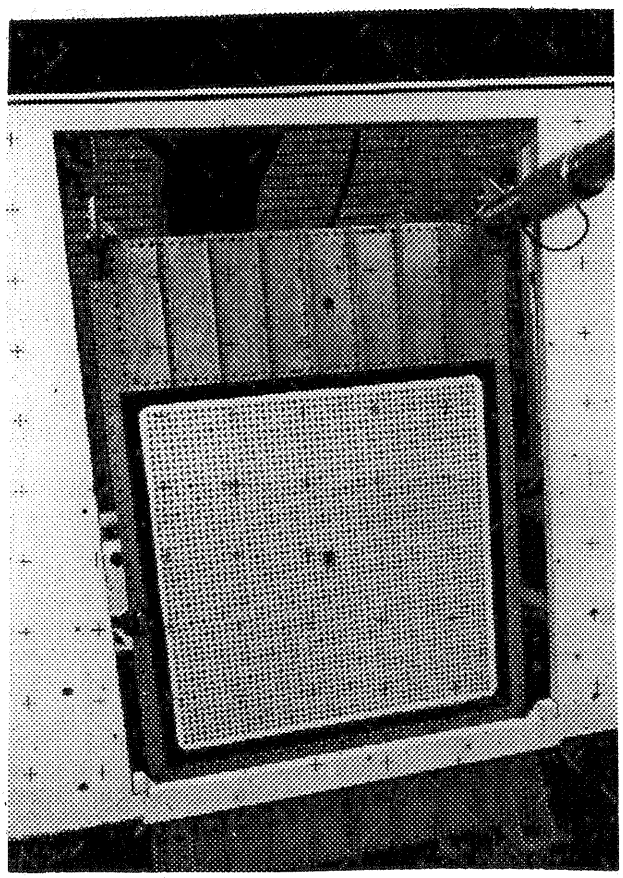

Figure 1 - The panel inserted in the loading machine

These sensors offer high accuracy and fast response to dynamic changes; their disadvantage is the relatively high cost (some hundreds may be necessary for a dense sampling of the deformations) and the calibration of the whole system. Another possibility is to create a series of

Moirè fringes on the structure, but the method may be used on a few points only and therefore is not suited for this application. Photogrammtry is on the contrary an ideal complement to strain gauges, since it provides with a dense field of 3D deformation vectors, allowing a precise reconstruction of the panel surface at any stage. In each loading sequence intermediate configurations may be recovered while the load is increased in steps. The initial panel shape must also be known, to derive the true boundary binding state and stress. The required accuracy in the direction normal to the panel surface was set in the order of 0.1 mm over the whole panel.

2. THE DESIGN OF THE SURVEY

Thanks to the simplicity of the task (no semantic involved, just mass point determination on a smooth, though very poorly textured, surface) the advantage of using an all digital solution (i.e. using digital cameras and automatic surface reconstruction) for the panel survey was self-evident. In principle, even a near real time solution might be achievable (though not required), if a sufficient number of cameras and enough computing power were available. We opted rather for a mixed approach, using an analogue camera for image acquisition, followed by scanning and processing of the digital images. The main reason for that choice was cost containment: since most of the funding allocated to the project was used to buy the loading machine, we were forced to use the cameras available to our Department, all of them still analogue metric or semimetric cameras. Given the accuracy goal, a standard digital camera would have required a more complex network design, while an high resolution camera would have been too expensive. For much the same reason, scanning has been performed by an inexpensive off-the-shelf DTP scanner, with maximum resolution of 800 dpi.
Even accounting for the additional burden given by the scanning process, performing the measurements automatically on digital images is clearly much faster than tackling the task by a human operator, hardly motivated by repeating thousends of times the same operation.
Among the available cameras, we choose the Rolleiflex 6006 with a 40 mm lens and a 11x11 reseau, for two main reasons:

- fast operation: in each static condition the load is maintained by an hydraulic system whose stability proved to be not very reliable; the shots relative to each loading stage should be therefore completed in a very short time, what is hard to achieve using metric cameras such as the Wild P31;
- scanner deformations: since our scanner may introduce considerable distortions, we preferred to be able to estimate corrections on each image, taking advantage of the reseau.

Simulations were carried out to determine the number of stations, the image scale and the degree of convergence of the camera axes. The main constraint on the design has been the reduced depth of field, which limited the minimum incidence angle to the object plane. We were also concerned of a possible decrease in the accuracy of l.s. matching in those areas where the perspective deformation heavily shrinks the target. Three basic configuration were selected, all of them consisting of 4 images, taken simmetrically, each covering the whole object (see figure 1):
- a normal case, with horizontal and vertical baselines of 40 cm and minimum distance to the object of 1.2 m;
- a slightly convergent case, with horizontal baseline of 120 cm and vertical baseline of 80 cm and same distance as above;
- a strongly convergent case, with horizontal baseline of 150 cm and vertical baseline of 70 cm, with minimum distance to the object of 70 cm.

Moreover, a fifth nadir image was taken to simplify the target localization procedure (see 5.).
Assuming an accuracy on the pixel coordinates of 1/20 of the pixel size, the photoscale would not have been enough to ensure the accuracy on object space at the maximum scanning resolution. The negatives where therefore enlarged by approximately a factor 2.5 and the printed copies digitized.
The panel surface is poorly textured and therefore correspondencies would be hard to find either for humans as well as for algorithms. A solution might have been using a light projector capable to create some pattern on the surface; we preferred instead to signalize the panel, making easier, if any, to compare pointwise the behaviour of the structure subject to different loading conditions and to use template matching rather than matching with respect to a reference image.
Taking into account the expected frequency components of the deformation surface, a regular square grid of targets (spaced 15 mm) was prepared on adhesive paper and fixed to the panel, totalling around 2700 point. The targets simply consist of a black circle with a diameter of 6 mm on a white background and have been prepared on a laser printer. Their size was computed, after selecting the photoscale and the scanning resolution, to ensure a target on average 20 pixel wide.

3. SCANNER CALIBRATION

As mentioned above, a UMAX UC840 Max Vision scanner has been used; its main the characteristic are as follows:
- scanning format: 216x356 mm; no transparency module;
- radiometric resolution: 8 bit;
- max optical geometric resolution: 400 dpi across scan, 800 dpi along scan direction; up to 1600 dpi in interpolated mode;
- internal buffer: 2 MB

The software driving the scanner allows for the standard grey value transformations (contrast, brightness, gamma correction, histogram equalization, etc.) and for freely defineble scanning area. In order to assess possible distorsions of the scanning process, radiometric and geometric properties of the scanner have been investigated.

3.1 Radiometry

The g.v. profile through the image of a target has been acquired at different times after the power was switched on. The maximum g.v. changes are in the order of 15% and occurred in the first minutes. The repeatability of the g.v. profile, after the warm-up effects vanish, is better than 1%.

A radiometric calibration has been performed by using a grey wedge chart; a certain non linearity and a loss of sensitivity in the dark region have been highlighted. To assess the influence on the target location by l.s.m., two tests have been carried out adjusting a block of 4 images with and without corrections: no significant changes to object coordinates have been found, therefore no corrections to g.v. were applied later.

3.2 Geometry

Since our scanner was not equipped with a transparency module, we could not use glass reseau plates. A simple reference grid was generated by cutting a reseau with a spacing of 1 cm on a 12x11 cm area (just larger than the size of our enlarged pictures) over a stable polyester film. The coordinates of the crosses were measured on a PK1 Zeiss comparator and, after scanning, by l.m.s. on the digital image, using an artificial template. The two sets of coordinates to compare are relative to reference systems which may differ either in orientation and scale (in two directions): an affine transformation has therefore been estimated, assuming as observations the pixel coordinates. Since the interior orientation will be performed by using the camera reseau crosses, the computed transformation parameters will not be used later. Nonetheless, it is interesting to look at the residuals of the affine, since they show deformations which will not be recovered by the transformation in the interior orientation.

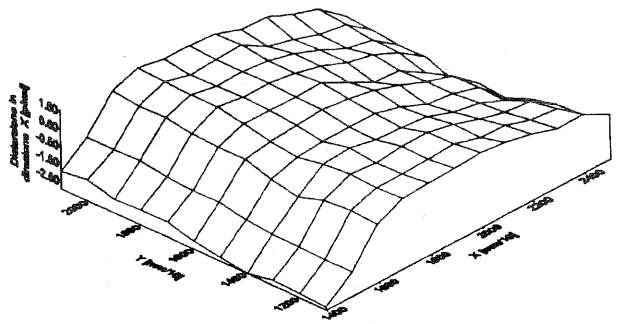

Figure 2 - Residuals of the X component (across scan)

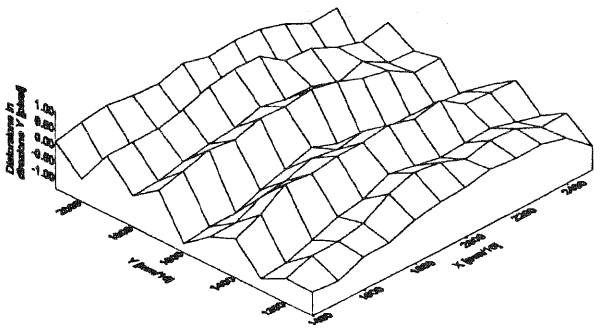

Figure 3 - Residuals of the Y component (along scan)

Figures 2 and 3 show the behaviour of the residuals of the X (across scan) and Y (along scan) components. It can be seen that distortions in X component are relatively uniform in Y direction, with a maximum value of about 3 pixels. Residuals of the Y component on the contrary show a wavy trend and are less predictable, but also smaller (up to 1 pixel) than the X component. They may be due to some irregularities in the movement of the optical system.
Another problem, occurring only when scanning large areas at high resolution, was perhaps due to the limits in memory (either of the scanner's buffer or of the PC's RAM): in such cases, the scan is completed in several stages, where the moving stage stops and then restart, after going back a few centimeters to reach the steady speed. In this operation losses up to ten rows have been noticed scanning a pattern of diagonal lines. In order to cope with this problem, thanks to the limited size of our images, we simply put them always in the calibrated area, where, at the selected resolution, the problem didn't show up.

4. INNER ORIENTATION

The transformation between pixel and image coordinates of the reseau crosses will partly adsorb the deformations due to scanning, to shrinkage of the negatives, to the enlargment and to the shrinkage of the enlarged copies. As outlined above, in principle we have at hand two sets of reference values: the results of the geometric calibration of the scanner and the coordinates of the camera reseau from the calibration certificate. The enlarged pictures proved to be sensitive to lack of orthogonality of the optical axis of the projector's objective with respect to the stages carrying the original and the enlarged picture. In order to account for this fact and to combine both reference sets we opted for a 8 parameter transformation for the inner orientation, followed by an interpolation of the residuals with a polynomial function modelling the scan deformation of the X component (see figure 2) as follows:

$$u = a_1 x^3 + a_2 x^2 + a_3 xy + a_4 x + a_5 y + a_6$$
$$v = b_1 x^3 + b_2 x^2 + b_3 xy + b_4 x + b_5 y + b_6$$

The performance of this two stage procedure have been compared against a simpler one (applying the 8 parameter transformation only) in one of the block adjustment performed. Taking as performance index sigma naught and the rms of the residual on check points, it turned out that the double stage procedure was slightly worse than the single stage. This may perhaps be attributed to instability of the scanner, so that the calibration procedure should be repeated just before scanning. In the adjustment of all blocks therefore the simplest procedure has been used.

5. POINT TRANSFER AND TARGET LOCALIZATION

After digitization of the images, a combination of an automatic and an interactive approach was used to locate approximately the targets and the reseau crosses on the images for the subsequent refinement by l.s. matching.

- Targets were approximately localized in the nadir image by first applying a smoothing filter followed by Foerstner's interest operator: with appropriate

selection of the smoothing factor, of the size of the operator's window and of the threshold values of the roundness and size of the error ellipse, the targets are located with good accuracy, providing with their pixel coordinates. There are however exceptions, due to interference (overlapping) of reseau crosses with the targets (bad starting points, missing targets). Moreover, candidates may be found which are not targets (e.g. scratches, dust, other distinct features on the image); they will be eliminated in a later stage. From the calibration certificate we also got the position of all reseau crosses.

- Taking advantage of the simple panel shape, which still can be represented with good approximation by a plane even after loading deformations, we used a simple point transfer mechanism. The positions of the same 4 points (either targets or crosses) were measured on the screen in each image. Then, the computation of an 8-parameter transformation between the reference coordinates (either pixel or calibration) and the corresponding pixel coordinates provides the automatic transfer of all targets and reseau crosses, with an approximation always within the pull-in range of the l.s.matching; no transfer ambiguities have been noticed, thanks to the spacing between targets and smoothness of the deformation.

5.1 Template least squares matching

The approximate target coordinates have been refined by template l.s. matching. The geometric transformation used for the search window is an affine. Any of its parameters may be nevertheless constrained, adjusting the model to a simpler one (shift only, conformal transformation, etc) prior to the processing (no testing of significance and updating is performed in the iteration process). If the correlation coefficient at the end of the process is larger than a threshold (0.7 in the case), depending on the quality of the points to be matched, the result is accepted.

The l.s. matching adjustment is sensitive to outliers in the gray values, due e.g. to dust or scratches or to disturbances in the target background. In such cases, the solution may converge to a local minimum, enjoying at the same time a high correlation (see figure 4). To tackle this behaviour, the matching has been robustified introducing an outlier rejection procedure. As a very basic but also sometimes very effective idea we removed from the solution the contribution of all pixels with g.v. outside a given range; this works well in a controlled enviroment. Rather than using a robust adjustment method, a more conventional data snooping procedure has been used, rejecting all standardized residual larger than 4 in a certain iteration of the adjustment. The outliers rejection take place only after a certain degree of convergence is reached, since at the beginning radiometric differences between template and slave are likely to depend more on the approximate registration of the images than on image noise. Experiences have shown that the procedure may cause some instability (oscillations of the parameters in subsequent iterations) but that it is effective in reducing the bias in many (but not all) cases (see figure 5).

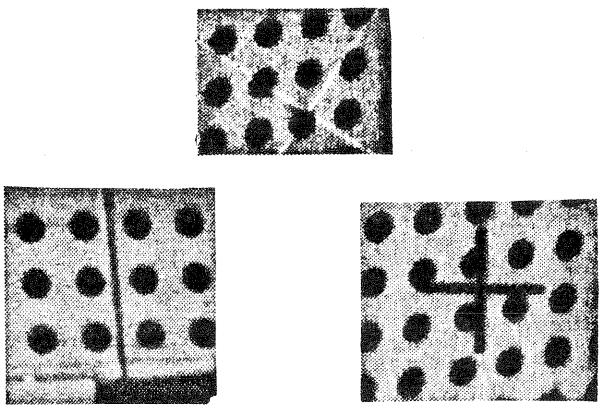

Figure 4 - Critical cases for l.s.m.

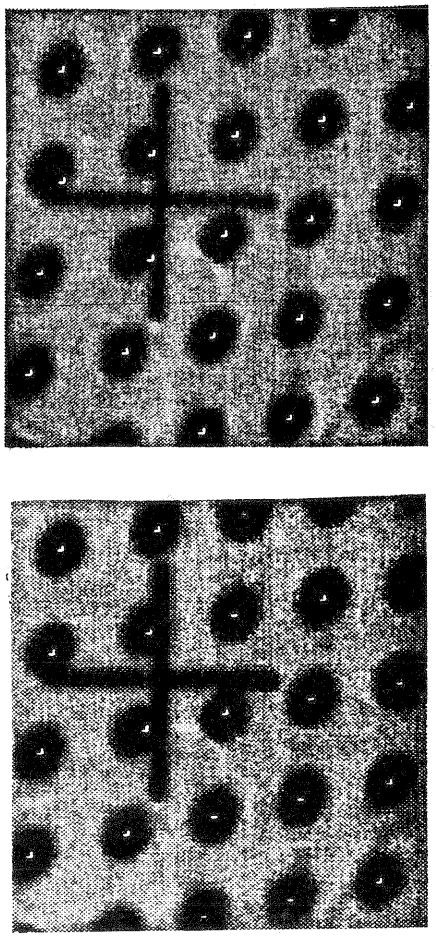

Figure 5 - The effect of the ouliers rejection procedure

The measurement of the crosses turned out to be very prone to disturbances due to dust, not to mention the overlap with the targets. To reduce these effects, the template used for the reseau represents only the core of the whole cross. In addition, only two bands of pixels along the cross arms are active, reducing the danger of interferences. This greatly improved the correlation coefficient and reduced the bias in the mesurements, thought not all crosses could be successfully matched and therefore used in the interior orientation.

To improve the fitting between template and search window, a radiometric transformation is introduced, which should partly compensate for differences in illumination, reflectivity and so on. The parameter of the transformation are not included in the l.s. adjustment, but

are computed prior to the matching, forcing the equalization of the mean and the variance of the g.v. between the two windows.

6. TOPOGRAPHIC CONTROL NETWORK AND PHOTOGRAMMETRIC SURVEY.

To avoid repeating the determination of ground control points after any change of the panel under study and to provide a stable reference for the various loading stages in a particular test, 9 control points were fixed on a granite frame surrounding the front of the loading machine and determined by forward intersection form three stations using a TC2000 Wild theodolite. Distances between the stations were measured by using a horizontal rod, which gives the highest accuracy on this range of distances (2-3 m). The accuracy of the control points turned out to be better than 0.1 mm in all coordinates.

Before entering the test sequence on the CFER panels, a preliminar survey was executed on an unloaded panel, to assess the whole procedure. Images were taken by the three configuration previously simulated and the pixel coordinates of the targets were measured by l.s.m. and then adjusted by bundles. The results of the three block adjustment are summarized in table 6.

It can be seen that the (theoretical) accuracy on the object depends more on the geometry of the intersection than on the accuracy of the l.s.m. on the image. Moreover, the accuracy on the image doesn't directly transfer to object coordinates, since the estimate for sigma naught is not proportional: this means that the distortions not adsorbed by the inner orientation are still important in determining the overall accuracy.

Bundle Adjustment Results	Nadir images	Slightly convergent images	Strongly convergent images
Height accuracy rms(SD) [mm]	0.21	0.13	0.07
σ_0 [μm]	4.3	5.2	3.6
Target accuracy rms(SD) [μm]	0.75	0.80	1.40

Table 6 - Bundle adjustment results in the three different image configuration.

After this pilot test, all subsequent surveys were carried out with the third configuration, using a focusing distance of 1.09 m and an aperture of f/11.

7. CONCLUSIONS

Many different tests have been carried out up to now on different panels and in all cases the surface deformations has been determined with an accuracy better than 0.1 mm.

The method proved to be very helpful to test the deformation predicted by finite elements: in most cases the results were in fact in agreement (see fig. 7), but in some others there were unexpected differences, showing that a more refined model should be used.

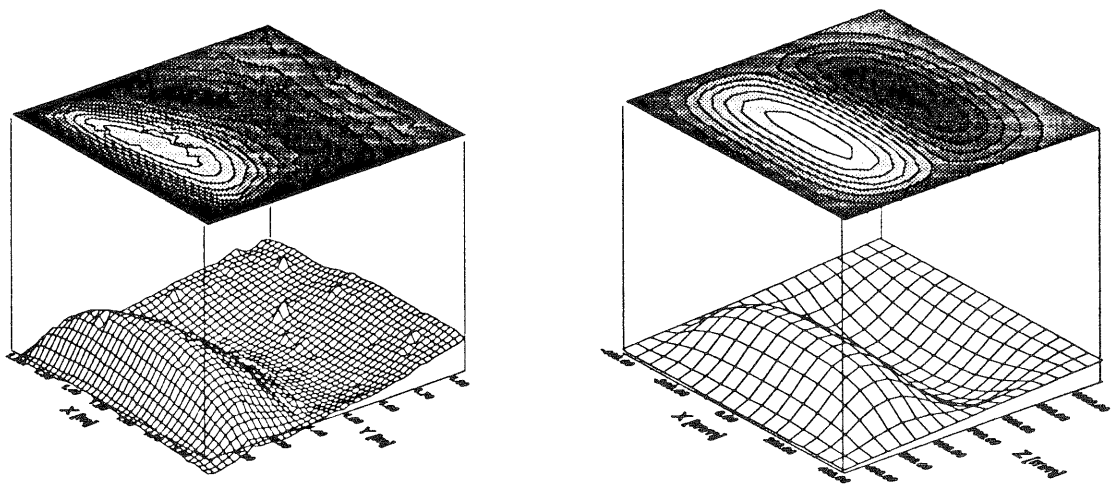

Figure 7 - Actual and expected deformation surface for a bending test.

After the first series of tests with the unloaded panel, the processing of all subsequent tests has been carried out, after some necessary training, by students without a specific background in photogrammetry, demonstrating an overall good level of user friendness of the system.

As far as the measurement of targets and reseau crosses by l.s.m. is concerned, some improvements are desirable. The outlier rejection is clearly still too weak in many cases, leading to biases in the image coordinates: a solution may be to try with robust adjustment methods or, in alternative, to use the redundancy of the scheme in a geometrically constrained matching environment. The point transfer procedure, though requiring a moderate interaction and clearly being successfull thanks to the simplicity of the object shape, seems more than appropriate to the task. We hope to move soon to an all digital system; in the meantime a combination of analog and digital still does his job.

References from Journals:
Bursi, O., Guzzetti, F., 1990. Photogrammetric survey and definition of failure mechanisms of bean-to-column steel connections. Costruzioni metalliche, 5, pp. 311-338.

References from Other Literature:
Baltsavias, E.P., 1994. Test and calibration procedures for image scanners. In: International Archives of Photogrammetric and Remote Sensing, Como, Italy, Vol. 30, Part 1, pp. 163-170.

Baltsavias, E.P., 1994. The AGFA HORIZON scanner characteristics, testing and evaluation. In: International Archives of Photogrammetric and Remote Sensing, Como, Italy, Vol. 30, Part 1, pp. 171-179.

Baltsavias, E.P., Bill, R., 1994. Scanners - A survey of current technology and future needs. In: International Archives of Photogrammetric and Remote Sensing, Como, Italy, Vol. 30, Part 1, pp. 130-143.

Baltavias, E.P., 1991. Multiphoto geometrically constrained matching. Institute of Geodesy and Photogrammetry, Swiss Federal Institute of Thechnology, Zurich, Switzerland, Mitteilungen n.49.

Crippa, B., De Haan, A., Forlani, G., 1993. Automatic deformation measurements from digital images. In: Optical 3-D measurement techniques II, Gruen-Kahmen (ed's), Wichman Verlag, Karlsruhe, pp. 557-563.

Förstner, W., 1986. A feature based correspondence algorithm for image matching. In: International Archives of Photogrammetric and Remote Sensing, Rovaniemi, Finland, Vol. 26, Part 3/3, pp. 150-166.